Pressure-correlated dispersion of inertial particles in free shear flows

Kun Luo, Jianren Fan,* and Kefa Cen
State Key Laboratory of Clean Energy Utilization, Zhejiang University, Hangzhou 310027, People's Republic of China
(Received 27 April 2006; revised manuscript received 23 December 2006; published 26 April 2007)

We investigate the relationship between dispersion of inertial particles and the pressure field in free shear flows. A three-dimensional temporally developing particle-laden mixing layer and a three-dimensional spatially developing particle-laden plane jet are studied by means of direct numerical simulation. The incompressible Navier-Stokes equations are accurately solved without any turbulence model. The dispersed inertial particles are traced in the Lagrangian framework. It is found that the instantaneous spatial distribution of inertial particles correlates well with the Laplacian of pressure $\nabla^2 p$, and from the statistical viewpoint, the effect of particle size on the fraction of particle number distributed within different flow zones characterized by $\nabla^2 p$ for different particles is negligible when the flow is well developed. The potential explanations and applications for this feature are explored.

DOI: 10.1103/PhysRevE.75.046309 PACS number(s): 47.55.Kf, 47.27.ek, 47.61.Jd

INTRODUCTION

Particle-droplet-bubble-laden turbulent flows exist widely in nature and in engineering application systems, ranging from atmospheric currents, dust storms, and spray combustion to plant-seed dispersal, aerosol deposition, and pollutant transport. It attracts both physicists and engineers to develop reliable theory and model to predict dispersion and transport of dispersed particles in various flows [1–3]. As to the dispersion of inertial particles in turbulent flows, a variety of phenomena have been observed, such as turbophoresis [4], preferential concentration [5], turbulent thermal diffusion-barodiffusion [6,7], focusing [8,9], anomalous scales [10], self-excitation and intermittent distribution [11,12], fractal and multifractal clustering [13,14], etc. Recently, particle dispersion in complex conditions has also been investigated [15–18]. In spite of great achievements [19,20], it is still a challenging task to put forward a universal predictive theory and model which is useful for engineering applications and also capable in quantifying various effects and phenomena mentioned above. For example, the preferential concentration of particles in turbulence is well known for a long time, but there is no state-of-the-art gas-solid two-phase model which can describe and predict it to the author's knowledge.

Towards this direction, this paper examines the pressure-correlated particle dispersion in free shear flows. The fluid motions are accurately solved by using direct numerical simulations (DNS). The dispersed inertial particles are traced in the Lagrangian framework. It is observed that the spatial dispersion of particles correlates well with the Laplacian of pressure $\nabla^2 p$, but the effect of particle size on the fraction of particle number distributed within different flow zones is negligible. To demonstrate this feature, a three-dimensional (3D) temporally developing particle-laden mixing layer and a three-dimensional spatially developing particle-laden jet are investigated, respectively. The potential explanation and the related applications are also discussed.

*Corresponding author. Electronic address: fanjr@zju.edu.cn

THREE-DIMENSIONAL PARTICLE-LADEN MIXING LAYER

In DNS of the particle-laden mixing layer, the pseudospectral method is used to solve the incompressible Navier-Stokes equations

$$\frac{\partial u_i}{\partial x_i} = 0, \tag{1}$$

$$\frac{\partial u_i}{\partial t} + \frac{\partial u_i u_j}{\partial x_j} = -\frac{1}{\rho}\frac{\partial p}{\partial x_i} + \frac{1}{\mathrm{Re}}\frac{\partial}{\partial x_j}\left(\frac{\partial u_i}{\partial x_j} + \frac{\partial u_j}{\partial x_i}\right). \tag{2}$$

The Reynolds number is defined as $\mathrm{Re}=U_0\theta_0/\nu=250$, where $U_0=(U_1-U_2)$ is the difference between two parallel streams, and θ_0 is the initial momentum thickness.

The trajectories of particles are traced using a Lagrangian tracking solver. Because of larger density ratio ($\rho_p/\rho_f=2000$), the pressure gradient, virtual mass, Basset and other possible forces can be neglected. Considering only the Stokes drag force, the nondimensional governing equation for the particle can be written as [21]

$$\frac{d\boldsymbol{V}}{dt} = \frac{f}{\mathrm{St}}(\boldsymbol{U}-\boldsymbol{V}), \tag{3}$$

where $\boldsymbol{V}$ is the particle velocity vector, $\boldsymbol{U}$ is the fluid velocity vector at the position of the particle, and f is the modification factor for the Stokes drag force. The particle Stokes number is defined as $\mathrm{St}=\frac{\rho_p d_p^2/18\mu}{\theta_0/U_0}$. Initially, the particles are uniformly distributed in the whole flow field. The flow configuration, boundary conditions, and numerical method are described in detail in previous literature [21,22].

On identification of coherent structures in turbulence, Dubief and Delcayre [23] reported that Q-isosurface is a better criterion. Q is defined as $Q=\frac{1}{2}(\Omega_{ij}\Omega_{ij}-S_{ij}S_{ij})$, where $\Omega_{ij}=\frac{1}{2}\left(\frac{\partial u_i}{\partial x_j}-\frac{\partial u_j}{\partial x_i}\right)$ and $S_{ij}=\frac{1}{2}\left(\frac{\partial u_i}{\partial x_j}+\frac{\partial u_j}{\partial x_i}\right)$ are, respectively, the antisymmetric and the symmetric tensors. Q is related to the pressure p by $Q=\frac{1}{2\rho}\nabla^2 p$, where ρ is fluid density. Therefore, one can investigate the correlation between $\nabla^2 p$ and particle distribution to reveal the effects on particle dispersion by

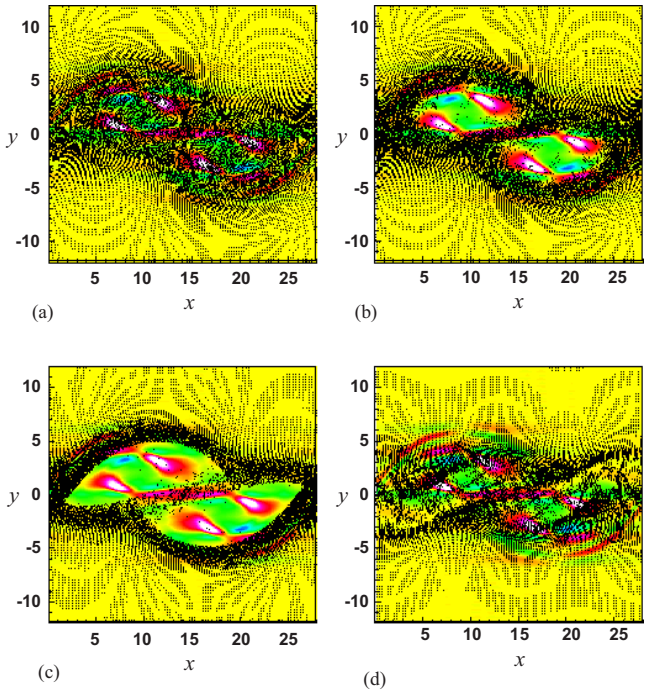

FIG. 1. (Color online) Spatial distribution of $\nabla^2 p$ and particles at St=0.01, 1, 10, and 100 in the plane $Z=T_z/4$ of the mixing layer at the nondimensional time $T=50$. (a) St=0.01, (b) St=1, (c) St=10, (d) St=100.

flow structures. Figure 1 shows the spatial distribution of $\nabla^2 p$ and the particles at St=0.01, 1, 10, and 100 in the plane $Z=T_z/4$ at the nondimensional time $T=50$. Colorized contours represent $\nabla^2 p$ and black points represent particles. It is observed that particle dispersion is closely related to the flow structures characterized by $\nabla^2 p$ and depends on the Stokes number. Particles at St=0.01 follow the fluid motion and are distributed uniformly. Particles at St=100 disperse less and directly pass through the flow structures. Particles at St=1 and 10 concentrate near the outer edges of the large-scale structures to form the quasicoherent particle dispersion structures. Although the distribution patterns of particles are similar to those of the previous studies [24,25], the figure demonstrates that particle dispersion correlates well with the Laplacian of pressure.

To further examine the relationship between particle dispersion and the pressure field, we statistically calculate the fraction of particle number distributed within different flow zones characterized by the Laplacian of pressure $\nabla^2 p$. Here the fraction of particle number, $\alpha(\nabla^2 p)$, is calculated as follows: (i) Choosing the lower and upper limit values of $\nabla^2 p$ as $(\nabla^2 p)_{\min}$ and $(\nabla^2 p)_{\max}$, (ii) subdividing the difference between $(\nabla^2 p)_{\max}$ and $(\nabla^2 p)_{\min}$ into n equally spaced slabs, (iii) counting the number of particles contained in each slab, (iv) dividing this number by the total number of particles in the flow field at a certain time, then $\alpha(\nabla^2 p)$ is obtained.

The fraction of particle number $\alpha(\nabla^2 p)$ for St=1 at different times is shown in Fig. 2. It is found that $\alpha(\nabla^2 p)$ correlates well with the Laplacian of pressure. The value of $\alpha(\nabla^2 p)$ is higher when $\nabla^2 p$ is close to 0 and decreases with the increasing of the absolute value of $\nabla^2 p$, which suggests

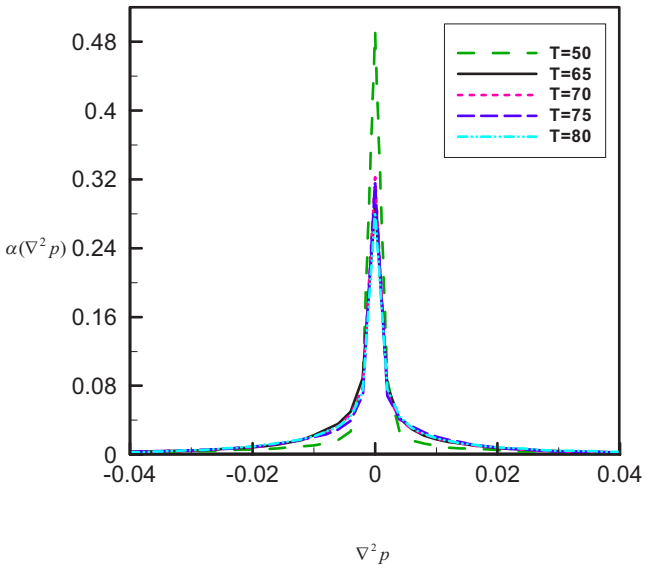

FIG. 2. (Color online) Fraction of particle number distributed within different flow zones characterized by $\nabla^2 p$ for particles at the Stokes number of 1 in the mixing layer at different times.

that a large percentage of particles tend to lie in the regions where no flow structures are observed [26], i.e., where the rotation rate $\Omega_{ij}\Omega_{ij}$ and the strain rate $S_{ij}S_{ij}$ are in balance. Compared with the $\nabla^2 p>0$ side, the value of $\alpha(\nabla^2 p)$ at $Q<0$ side is slightly higher. It indicates that the inertial particles preferentially concentrate in the regions of excess strain rate over rotation rate. This trend is consistent with the findings in the previous review [5]. When examining the variation of $\alpha(\nabla^2 p)$ with the time, an attractive phenomenon is observed. After $T>65$, the curves overlap each other so well that a single fitting curve can be used to represent the fraction of particle number at different times. It implies that the particle distribution becomes statistically time independent when the flow is developed enough, which is helpful for predicting particle dispersion in turbulent flows as stated later. Due to the fact that $\frac{1}{\rho}\nabla^2 p=\nabla\cdot\boldsymbol{a}$ where $\boldsymbol{a}$ is the fluid acceleration, the above results also indicate that the particle distribution is closely related to the fluid acceleration, which agrees well with recent studies [27–29].

Figure 3 shows $\alpha(\nabla^2 p)$ for different particles at $T=70$. It is found that the data for different kinds of particles collapse fairly well onto a single curve again. This means that the particle size has a negligible effect on $\alpha(\nabla^2 p)$ from the viewpoint of statistical sense when the flow is statistically steady, although the particle size does have predominant effects on the spatial distribution of particles and their distribution patterns also correlate well with $\nabla^2 p$. Similar to the present study, Lazaro and Lasheras [30] experimentally studied particle dispersion in an unforced free shear layer and found that the particle size has no effect on particle thickness and concentration profile when the flow was fully developed if a suitable characteristic length scale L_D was selected. Winkler *et al.* [31] investigated the preferential concentration of dense particles in a turbulent square duct flow using large eddy simulations. They selected vorticity magnitude, swirling strength, maximum compressional strain rate, $\nabla\mathbf{u}:\nabla\mathbf{u}$

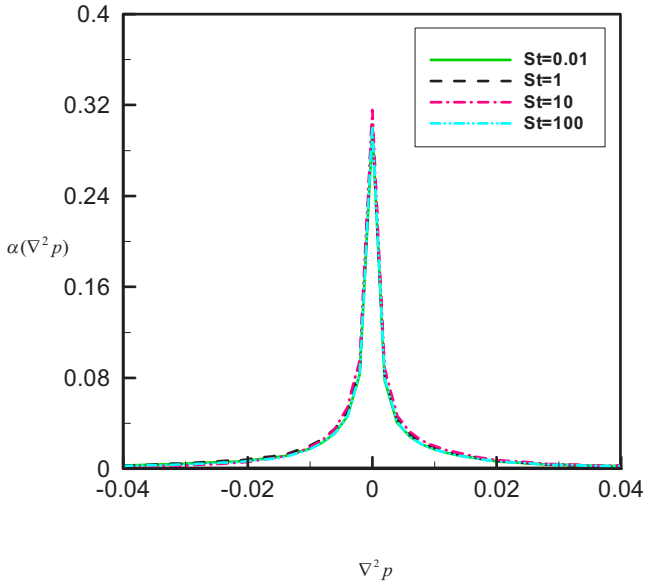

FIG. 3. (Color online) Fraction of particle number distributed within different flow zones characterized by $\nabla^2 p$ for particles at different Stokes numbers in the mixing layer at the nondimensional time $T=70$.

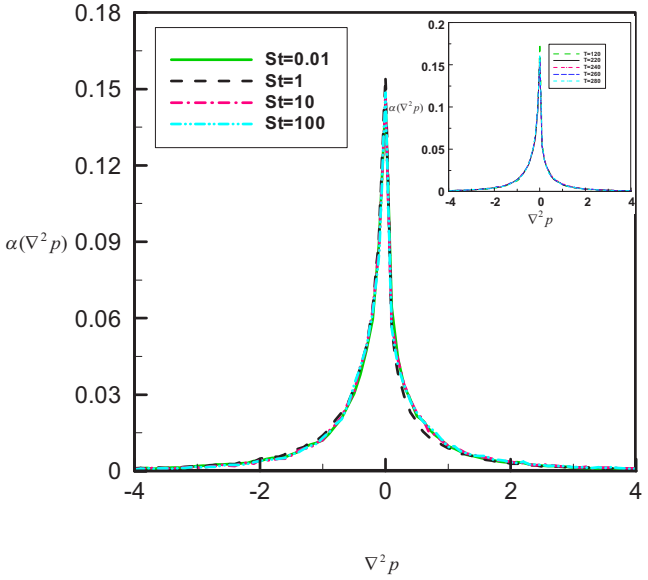

FIG. 4. (Color online) Fraction of particle number distributed within different flow zones characterized by $\nabla^2 p$ for particles at different Stokes numbers in the jet at the nondimensional time $T=240$. Inset: Fraction of particle number distributed within different flow zones characterized by $\nabla^2 p$ for particles at the Stokes number of 1 in the jet at different times.

$(-Q$ in the present study) and the cross-sectional location as the statistical variables. Although it was not directly pointed out in their study, one can conclude from their Fig. 25 that the PDFs of $-Q$ in the vortex center region for particles at the Stokes numbers of 0.25, 1.0, and 8.0 have negligible relation with the particle size. Furthermore, this size-independent property appears only for the parameter $-Q$ and only in the free vortex center region. The situations and the results are very similar to ours. These previous results support our present statements.

THREE-DIMENSIONAL PARTICLE-LADEN JET

For universality, the fraction of particle number distributed within different flow zones in a three-dimensional spatially developing particle-laden plane jet is also investigated based on DNS. The flow configuration is similar to previous two-dimensional simulations [9,32]. The Reynolds number Re, based on the nozzle width d and the inflow velocity U_0, is 4000. The incompressible Navier-Stokes equations are solved by finite volume method and fractional-step projection technique. The boundary conditions, numerical algorithms, and code validation can be found in Refs. [33,34]. Inertial particles are traced in the Lagrangian framework considering only the Stokes drag force. The nondimensional governing equation for particle motion is the same as Eq. (3). Here the Stokes number is defined as $\mathrm{St}=\frac{\rho_p d_p^2/(18\mu)}{d/U_0}$.

As can be seen from Fig. 4, the fraction of particle number $\alpha(\nabla^2 p)$ for different particles correlates well with $\nabla^2 p$ and the curves overlap each other at $T=240$. It suggests that although the parameter $\nabla^2 p$ has important effects on $\alpha(\nabla^2 p)$, the effect of particle size on it is also negligible in the spatially developing plane jet when the flow is developed enough. Compared with Fig. 3, the shape of the curves is similar, but the peak value is lower and the bias toward the $\nabla^2 p<0$ side is more remarkable in the jet. The difference is associated with the different flow configurations. In the temporally developing mixing layer, the particles are initially distributed uniformly in the whole field and only two roller structures are observed. But in the spatially developing jet, the particles are released just at the nozzle and more roller and pairing structures are captured. Thus more particles lie in the regions characterized by flow structures and the preferential concentration in the low-vorticity and high-strain regions is more apparent. In the inset, the fraction of particle number $\alpha(\nabla^2 p)$ for particles at $\mathrm{St}=1$ is plotted. It can also be seen that the time has a negligible effect on $\alpha(\nabla^2 p)$ after nondimensional time $T>200$. Indeed, we find that the jet becomes statistically steady after $T>200$ in our simulations.

Although the particle size has a negligible effect on the fraction of particle number distributed within different flow zones characterized by the Laplacian of pressure $\nabla^2 p$ as shown above, it has a distinct effect on some other statistical quantities. As indicated in Fig. 5, the mean interphase slip velocity $|\boldsymbol{U}\text{-}\boldsymbol{V}|$ is low in the zones of $\nabla^2 p\approx 0$ but particles at the larger Stokes number have the relatively higher values of $|\boldsymbol{U}\text{-}\boldsymbol{V}|$. With the increasing of the absolute value of $\nabla^2 p$, $|\boldsymbol{U}\text{-}\boldsymbol{V}|$ becomes higher and higher, but the larger Stokes number results in the relatively lower value of it.

DISCUSSIONS

The above results demonstrate that the spatial distribution of particles at different Stokes numbers correlates well with the Laplacian of pressure $\nabla^2 p$, and the effect of particle size on the fraction of particle number distributed within different

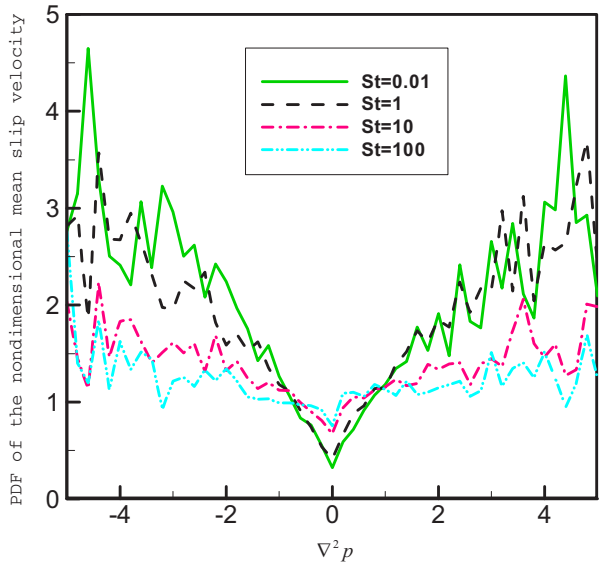

FIG. 5. (Color online) Distribution of mean interphase slip velocity in different flow zones characterized by $\nabla^2 p$ for particles at different Stokes numbers in the plane jet at the nondimensional time $T=260$.

flow zones in the free shear flows is negligible when the flow is developed enough. The mechanism for the passive particles can be easily concluded based on the previous studies [35,36]. To further explore the potential explanation for heavy inertia particles, we expand the definition of the fraction of particle number as follows:

$$\alpha(\nabla^2 p) = \frac{N_p(\nabla^2 p)}{N_p} = \frac{\sum_{\Omega(\nabla^2 p)} n(\boldsymbol{x},t)\Delta x\Delta y\Delta z}{\sum_{\Omega} n(\boldsymbol{x},t)\Delta x\Delta y\Delta z} = \frac{\overline{n(\boldsymbol{x},t)}_l N_f(\nabla^2 p)}{\overline{n(\boldsymbol{x},t)} N_f}, \tag{4}$$

where $N_p(\nabla^2 p)$ and $N_f(\nabla^2 p)$ are, respectively, the particle number and computational grid number contained in the zone characterized by $\nabla^2 p$; N_p and N_f are, respectively, the total particle number and total computational grid number in the flow field; $\Omega(\nabla^2 p)$ and Ω, respectively, represent the domain characterized by $\nabla^2 p$ and the whole computational domain. $n(\boldsymbol{x},t)$ is the local particle number density, $\overline{n(\boldsymbol{x},t)}_l$ is the mean particle number density over the local domain, and $\overline{n(\boldsymbol{x},t)}$ is the mean particle number density over the whole domain. The above expressions show that if $\overline{n(\boldsymbol{x},t)}_l = \overline{n(\boldsymbol{x},t)}$ then $\alpha(\nabla^2 p)$ is degenerated into the probability distribution of $\nabla^2 p$ which is the flow property, of course independent of the particle size and the time when the flow is developed enough. The condition $\overline{n(\boldsymbol{x},t)}_l \approx \overline{n(\boldsymbol{x},t)}$ is easily satisfied for particles at small and large Stokes numbers because their spatial distribution is approximately uniform. At small Stokes numbers the particles just follow the incompressible flow, while at large Stokes numbers their motion is more and more ballistic, as shown in Fig. 1. For Stokes numbers near unity, the particle distribution is not uniform. But when the flow is well developed, the locally mean particle number density is expected to approach the whole mean particle number density in the considered situations. Based on these facts, the curves for $\alpha(\nabla^2 p)$ at different Stokes numbers are very close to each other, as demonstrated above.

This feature can provide ideas both for the development of theoretical models and for the engineering applications. For example, if we get $\nabla^2 p$ by solving the fluid equations, we can predict the distribution of particle concentration in the flow according to the correlation between $\nabla^2 p$ and $\alpha(\nabla^2 p)$ without solving the particle equations. Or if we get the pressure distribution, which usually can be more easily measured than other parameters, we can predict the concentration distribution of particles. But the universal expression for the correlation between pressure and particle concentration in free shear flows still needs to be explored. More experimental and numerical studies are also necessary to validate the point.

ACKNOWLEDGMENTS

The authors would like to thank Dr. Markus Klein for his help and discussions. The authors acknowledge one of the anonymous reviewers for many insightful comments which greatly improved this paper. The authors also are grateful for the support of this research by the National Natural Science Foundation of China (Grants Nos. 50506027 and 50236030).

[1] R. Nathan *et al.*, Nature (London) **418**, 409 (2002).
[2] G. Falkovich, A. Fouxon, and M. G. Stepanov, Nature (London) **419**, 151 (2002).
[3] Z. Levin, S. Wurzler, and T. Reisin, J. Geophys. Res. **105**, 4501 (2000).
[4] M. Caporaloni *et al.*, J. Atmos. Sci. **32**, 565 (1975).
[5] J. K. Eaton and J. R. Fessler, Int. J. Multiphase Flow **20**, 169 (1994).
[6] T. Elperin, N. Kleeorin, and I. Rogachevskii, Phys. Rev. Lett. **76**, 224 (1996).
[7] R. V. R. Pandya and F. Mashayek, Phys. Rev. Lett. **88**, 044501 (2002).
[8] T. Shinbrot, M. M. Alvarez, J. M. Zalc, and F. J. Muzzio, Phys. Rev. Lett. **86**, 1207 (2001).
[9] J. R. Fan, K. Luo, M. Y. Ha, and K. Cen, Phys. Rev. E **70**, 026303 (2004).
[10] T. Elperin, N. Kleeorin, and I. Rogachevskii, Phys. Rev. E **58**, 3113 (1998).
[11] T. Elperin, N. Kleeorin, and I. Rogachevskii, Phys. Rev. Lett. **77**, 5373 (1996).
[12] E. Balkovsky, G. Falkovich, and A. Fouxon, Phys. Rev. Lett. **86**, 2790 (2001).
[13] J. Bec, Phys. Fluids **15**, L81 (2003).
[14] J. Bec, K. Gawedzki, and P. Horvai, Phys. Rev. Lett. **92**,

224501 (2004).
[15] S. V. Apte *et al.*, Int. J. Multiphase Flow **29**, 1311 (2003).
[16] R. V. R. Pandya, P. Stansell, and J. Cosgrove, Phys. Rev. E **70**, 025301(R) (2004).
[17] W. C. Reade and L. R. Collins, Phys. Fluids **12**, 2530 (2000).
[18] A. Keswani and L. R. Collins, New J. Phys. **6**, 119 (2004).
[19] G. Falkovich, K. Gawedzki, and M. Vergassola, Rev. Mod. Phys. **73**, 913 (2001).
[20] F. Mashayek and R. V. R. Pandya, Prog. Energy Combust. Sci. **29**, 329 (2003).
[21] W. Ling *et al.*, J. Fluid Mech. **358**, 61 (1998).
[22] J. R. Fan, K. Luo, Y. Zheng, H. Jin, and K. Cen, Phys. Rev. E **68**, 036309 (2003).
[23] Y. Dubief and F. Delcayre, J. Turbul. **1**, 011 (2000).
[24] C. T. Crowe, T. N. Chung, and T. R. Troutt, Part. Sci. Technol. **3**, 149 (1985).
[25] E. K. Longmire and J. K. Eaton, J. Fluid Mech. **236**, 217 (1992).
[26] M. S. Chong, A. E. Perry, and B. J. Cantwell, Phys. Fluids A **2**, 765 (1990).
[27] L. Chen, S. Goto, and J. C. Vassilicos, J. Fluid Mech. **553**, 143 (2006).
[28] J. Bec *et al.*, e-print nlin.CD/0608045.
[29] S. Goto and J. C. Vassilicos, New J. Phys. **6**, 65 (2004).
[30] B. J. Lazaro and J. C. Lasheras, J. Fluid Mech. **235**, 143 (1992).
[31] C. M. Winkler, S. L. Rani, and S. P. Vanka, Int. J. Multiphase Flow **30**, 27 (2004).
[32] K. Luo, J. R. Fan, and K. F. Cen, Proc. R. Soc. London, Ser. A **461**, 3279 (2005).
[33] M. Klein, A. Sadiki, and J. Janicka, Int. J. Heat Fluid Flow **24**, 785 (2003).
[34] K. Luo *et al.*, Phys. Lett. A **357**, 345 (2006).
[35] M. R. Maxey, J. Fluid Mech. **174**, 441 (1987).
[36] Y. Zhou, A. S. Wexler, and L. P. Wang, Phys. Fluids **10**, 1206 (1998).